Cooperative Maximum Likelihood Target Position Estimation for MIMO-ISAC Networks

Lorenzo Pucci, *Member, IEEE*, Tommaso Bacchielli, *Graduate Student Member, IEEE*, and Andrea Giorgetti, *Senior Member, IEEE*

Abstract—This letter investigates target position estimation in integrated sensing and communications (ISAC) networks composed of multiple cooperating monostatic base stations (BSs). Each BS employs a MIMO-orthogonal time-frequency space (OTFS) scheme, enabling the coexistence of communication and sensing. A general cooperative maximum likelihood (ML) framework is derived, directly estimating the target position in a common reference system rather than relying on local range and angle estimates at each BS. Positioning accuracy is evaluated in single-target scenarios by varying the number of collaborating BSs, using root mean square error (RMSE), and comparing against the Cramér-Rao lower bound. Numerical results demonstrate that the ML framework significantly reduces the position RMSE as the number of cooperating BSs increases.

Index Terms—ISAC, cooperative sensing, maximum likelihood, Cramér-Rao lower bound, OTFS.

I. Introduction

THE emergence of integrated sensing and communication ▲ (ISAC) as a paradigm for future mobile networks has opened new possibilities for joint environmental sensing and communication. In this context, cooperative multi-BS strategies are gaining traction for enhancing object localization and tracking capabilities [1]. Recent studies have focused on cooperative ISAC system, particularly in base station (BS) selection and resource optimization [2]–[6]. For instance, [2] proposes a BS selection method and assesses cooperative localization against theoretical bounds. In [3], symbol-level fusion of orthogonal frequency-division multiplexing (OFDM) echo signals acquired from different BSs enables effective cooperative distance and velocity estimation. A Pareto optimization framework is introduced in [4] to evaluate the tradeoff between the sum rate of multiple communication users and the positioning error bound of radar targets in ISAC systems.

Despite the growing interest in collaborative sensing, a gap remains in deriving a closed-form expression for cooperative maximum likelihood (ML) target position estimation based on the joint processing of signals received at different BS. To address this, we propose a cooperative ISAC system utilizing orthogonal time frequency space (OTFS) modulation with multiple monostatic multiple-input multiple-output (MIMO) BSs. Specifically, we present a general ML framework for

This work was supported by the European Union - Next Generation EU under the Italian National Recovery and Resilience Plan (NRRP), Mission 4, Component 2, Investment 1.3, partnership on "Telecommunications of the Future" (PE00000001 - program "RESTART"). The authors are with the Wireless Communications Laboratory, CNIT, DEI, University of Bologna, Italy, Email: {lorenzo.pucci3, tommaso.bacchielli2, andrea.giorgetti}@unibo.it

target position estimation, wherein signals from each BS are processed at a fusion center, and the target position is estimated relative to a common reference system. Additionally, we derive the cooperative position error bound (PEB) for the networked OTFS-based system, which serves as a theoretical lower bound for positioning accuracy. Through numerical simulations, we demonstrate that BS cooperation, based on ML estimation, significantly improves localization accuracy—often achieving multi-fold improvements compared to single BS configurations—and validate the ML estimation against the PEB.

In this letter, capital and lowercase bold letters represent matrices and vectors, respectively; $(\cdot)^T$, $(\cdot)^H$, and $\|\cdot\|$ denote transpose, conjugate transpose, and Euclidean norm, respectively; $\{\mathbf{a}_i\}_{i=1}^N$ denotes a vector $\mathbf{a} = [a_1, \ldots, a_N]$; \mathbf{I}_n is the $n \times n$ identity matrix, and $\mathrm{Tr}(\cdot)$ represents the trace of a matrix; $\mathbb{E}\{\cdot\}$ and $\mathbb{V}\{\cdot\}$ denote the mean value and variance, respectively; $\mathbf{x} \sim \mathcal{CN}(\mathbf{0}, \mathbf{\Sigma})$ represents a zero-mean circularly symmetric complex Gaussian vector with covariance $\mathbf{\Sigma}$; $\mathfrak{Re}\{\cdot\}$ and $|\cdot|$ represent the real part and absolute value, respectively, of a complex number, and \otimes represents the Kronecker product.

The rest of the letter is organized as follows. Section II presents the system model, Section III derives the cooperative ML estimation framework and the Cramér-Rao lower bound (CRLB), Section IV provides numerical results, and Section V concludes the letter with remarks.

II. SYSTEM MODEL

A. Physical Model

This work considers an OTFS-based network, where several monostatic MIMO BSs, each equipped with an ISAC transceiver with $N_{\rm T}$ transmit and $N_{\rm R}$ receive antennas, cooperate through a fusion center to localize targets within a designated region, as schematically shown in Fig. 1. Each BS can split sensing and communication in a time- or frequency-division manner based on the required quality of service.

Each OTFS system operates at a given carrier frequency f_c , with a bandwidth $B = M\Delta f \ll f_c$, where M is the number of subcarriers and $\Delta f = 1/T$ is the subcarrier spacing, with T being the time slot duration.¹

Consider a scenario with P point-like targets, each moving with a radial velocity v_p at a distance r_p from the monostatic transceiver and with radar cross-section σ_p . Assuming far-field line of sight (LoS) propagation between the transceiver and

¹Note that different BSs on the same network are coordinated to prevent mutual interference.

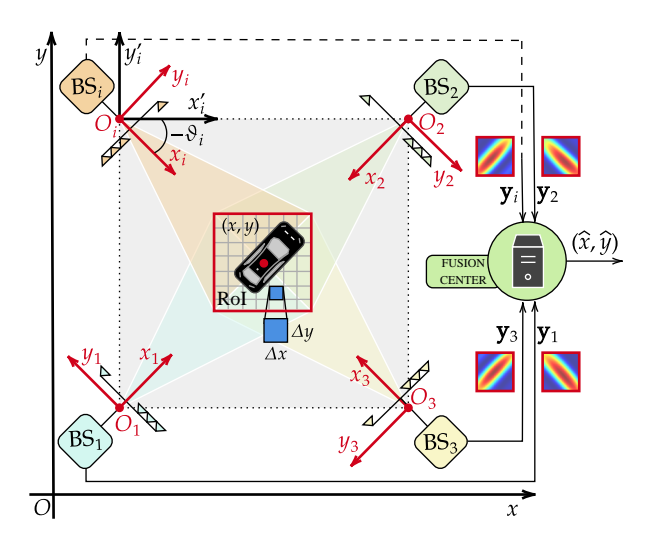


Fig. 1. Schematic representation of a network of $N_{\rm bs}$ cooperating BSs for target localization. The red square indicates the RoI where fine-grained grid ML target parameter estimation is performed.

each target, the $N_{\rm R} \times N_{\rm T}$ complex baseband channel impulse response of the radar function is expressed as

$$\mathbf{H}(t,\tau) = \sum_{p=0}^{P-1} \alpha_p \mathbf{b}(\phi_p) \mathbf{a}^{\mathsf{H}}(\phi_p) \delta(\tau - \tau_p) e^{j2\pi f_{\mathbf{D},p}t}$$
(1)

where α_p is the complex channel gain, accounting for attenuation and phase shift, $f_{\mathrm{D},p}=2v_pf_c/c$ represents the Doppler shift, and $\tau_p=2r_p/c$ is the round-trip delay, with c denoting the speed of light. According to the radar equation, $|\alpha_p|^2=\frac{G^2\sigma_p\,c^2}{(4\pi)^3\,f_c^2\,r_p^4},$ where G^2 accounts for the single antenna element gain G of the transmitter (Tx) and receiver (Rx) arrays. Furthermore, $\mathbf{a}(\phi_p)$ and $\mathbf{b}(\phi_p)$ denote the Tx and Rx array response vectors associated with the p-th target, with ϕ_p the p-th angle of departure (AoD)/angle of arrival (AoA), assumed to be equal in the monostatic setup. For uniform linear arrays (ULAs) with N_{T} antenna elements spaced at half-wavelength intervals, the array response vector is given by $\mathbf{a}(\phi_p)=[e^{-j\frac{N_{\mathrm{T}}-1}{2}\pi\sin\phi_p},\ldots,e^{j\frac{N_{\mathrm{T}}-1}{2}\pi\sin\phi_p}]^{\mathrm{T}}$. The same definition applies to $\mathbf{b}(\phi_p)$ with N_{R} .

B. OTFS-ISAC Input-Output Relationship

Considering a total of N time slots, the vector of signals transmitted through the $N_{\rm T}$ antennas at the n-th time slot is

$$\mathbf{s}_n(t) = \sqrt{P_{\text{avg}}} \sum_{m=0}^{M-1} X[n, m] \mathbf{w}_{\text{T}} e^{j2\pi m\Delta f(t-nT)} g_{\text{tx}}(t - nT)$$
(2)

where $P_{\mathrm{avg}} = P_{\mathrm{T}}/M$ is the average transmit power per subcarrier with P_{T} the total transmit power dedicated to sensing. The vector \mathbf{w}_{T} represents the unit-norm beamforming vector, chosen to provide nearly constant gain over a given circular sector, following the approach outlined in [7]. The pulse shape is represented by $g_{\mathrm{tx}}(t)$ and $X[n,m] \in \mathbb{C}$ is the complex symbol located in the $N \times M$ time-frequency domain grid obtained via symplectic finite Fourier transform (SFFT) from complex data symbols $x[k,l] \in \mathcal{A}$, where \mathcal{A} is

the complex alphabet and $\mathbb{E}\{|x[k,l]|^2\}=1$, arranged in the $M\times N$ delay-Doppler domain grid, i.e.,

$$X[n,m] = \frac{1}{\sqrt{NM}} \sum_{k=0}^{M-1} \sum_{l=0}^{N-1} x[k,l] e^{-j2\pi(\frac{mk}{M} - \frac{nl}{N})}$$
(3)

with n, l = 0, ..., N - 1 and m, k = 0, ..., M - 1. Further details on the processing chain are available in [8]–[10].

The transmitted signal s(t), after the channel (1), is collected at each Rx antenna and processed by a filter matched to the demodulating pulse $g_{\rm rx}(t)$. In the ideal case of biorthogonality between transmitting and receiving pulses for integer multiples of T and Δf , inter-symbol interference (ISI) can be avoided without a cyclic prefix (CP). However, in the more realistic scenario of imperfect bi-orthogonality, as considered here, some residual ISI occurs without a CP [8]. The output of the matched filter is then sampled at t = nT and $f = m\Delta f$, forming a $N \times M$ symbol grid in the time-frequency domain, whose (n,m) element is [8]

$$Y[n,m] = \sum_{n'=0}^{N-1} \sum_{m'=0}^{M-1} X[n',m'] \mathbf{h}_{n,m}[n',m'].$$
 (4)

The time-frequency domain channel vector, $\mathbf{h}_{n,m}[n',m']$, of size $N_{\mathrm{R}} \times 1$ is

$$\mathbf{h}_{n,m}[n',m'] \triangleq \sum_{n=0}^{P-1} h_p \mathbf{b}(\phi_p) e^{j2\pi n' T f_{\mathbf{D},p}} e^{-j2\pi m \Delta f \tau_p} \times$$

$$\times A_{g_{\text{rx}},g_{\text{tx}}} ((n-n')T - \tau_p, (m-m')\Delta f - f_{D,p})$$
 (5)

where $h_p \triangleq \sqrt{P_{\mathrm{avg}}} \, \gamma_p \, \alpha_p \, e^{j2\pi f_{\mathrm{D},p} \tau_p}$ is the overall complex channel factor, with the complex beamforming factor $\gamma_p = \mathbf{a}^{\mathrm{H}}(\phi_p)\mathbf{w}_{\mathrm{T}}$ related to the AoD of target p. The term $A_{g_{\mathrm{rx}},g_{\mathrm{tx}}}\left(\tau,f_{\mathrm{D}}\right)$ is the cross-ambiguity function between the two pulses $g_{\mathrm{rx}}(t)$ and $g_{\mathrm{tx}}(t)$, here both chosen to be rectangular pulses of duration T.²

Lastly, the demodulated symbols, back in the delay-Doppler domain, are obtained by performing inverse symplectic finite Fourier transform (ISFFT) on the symbols in (4), as [8], [9]

$$\mathbf{y}[k,l] = \sum_{p=0}^{P-1} h_p \mathbf{b}(\phi_p) \sum_{k'=0}^{M-1} \sum_{l'=0}^{N-1} x[k',l'] \mathbf{\Psi}_{l,l'}^p[k,k']$$
 (6)

where $\Psi^p \in \mathbb{C}^{MN \times MN}$ is a matrix retaining information on Doppler shift and round-trip delay for the p-th target. Under the hypothesis of rectangular pulses and a maximum channel delay smaller than T, an easy-to-handle expression of this matrix can be found in [9], [10].

Without loss of generality, we consider the presence of one target, i.e., P=1. Thus, through a vectorization operation

 $^2{\rm The}$ cross-ambiguity function between two generic pulses $g_u(t)$ and $g_v(t)$ is defined as [9]

$$A_{g_u,g_v}(\tau, f_{\mathrm{D}}) \triangleq \int_0^T g_u(t)g_v^*(t-\tau)e^{-j2\pi f_{\mathrm{D}}t}dt$$

$$\approx \frac{T}{M} \sum_{i=0}^{M-1} g_u\left(i\frac{T}{M}\right)g_v^*\left(i\frac{T}{M}-\tau\right)e^{-j2\pi f_{\mathrm{D}}i\frac{T}{M}}.$$

$$\mathbf{y} = h\mathbf{G}(f_{\mathrm{D}}, \tau, \phi)\mathbf{x} + \boldsymbol{\nu} \tag{7}$$

where $\mathbf{y} \in \mathbb{C}^{MNN_{\mathrm{R}} \times 1}$ contains the received symbols at each Rx antenna, $\boldsymbol{\nu} \sim \mathcal{CN}(\mathbf{0}_{MNN_{\mathrm{R}}}, \sigma_{\boldsymbol{\nu}}^2 \mathbf{I}_{MNN_{\mathrm{R}}})$ is the complex additive white Gaussian noise (AWGN) vector with $\sigma_{\boldsymbol{\nu}}^2 = N_0 \Delta f$, being N_0 the noise power spectral density, and $\mathbf{G} \in \mathbb{C}^{MNN_{\mathrm{R}} \times MN}$ the effective channel matrix given by [11]

$$\mathbf{G}(f_{\mathrm{D}}, \tau, \phi) \triangleq \mathbf{b}(\phi) \otimes \mathbf{\Psi}. \tag{8}$$

III. SENSING PARAMETERS ESTIMATION AND CRAMÉR-RAO LOWER BOUND

A. Cooperative Maximum Likelihood Position Estimation

Let us consider the scenario in Fig. 1, where $N_{\rm bs}$ BSs at coordinates $\mathcal{O}_i = [x_{\rm bs}^{(i)}, y_{\rm bs}^{(i)}]^{\rm T}$, with $i=1,\ldots,N_{\rm bs}$, cooperate to locate the point-like target at $\mathbf{p}=[x,y]^{\rm T}$ in a common Cartesian reference system. The target position in the local reference system centered at \mathcal{O}_i is given by $\mathbf{p}_i = [x_i,y_i]^{\rm T} = [r_i\cos(\phi_i),r_i\sin(\phi_i)]^{\rm T}$, with $r_i=\tau_i\,c/2$.

By collecting the backscattered signals by the *i*-th BS, \mathbf{y}_i , detailed in (7), the vector $\tilde{\mathbf{y}} \in \mathbb{C}^{MNN_{\mathrm{R}}N_{\mathrm{bs}}\times 1}$ of all received symbols is

$$\tilde{\mathbf{y}} = \begin{bmatrix} \mathbf{y}_1^\mathsf{T}, \mathbf{y}_2^\mathsf{T}, \dots, \mathbf{y}_{N_{b-1}}^\mathsf{T} \end{bmatrix}^\mathsf{T}.$$

The vector of target parameters to be estimated with respect to the *i*-th BS is $\boldsymbol{\theta}_i = [\beta_i, \varphi_i, f_{\mathrm{D},i}, \tau_i, \phi_i]^\mathsf{T}$, where $\beta_i = |h_i|$ and $\varphi_i = \angle h_i$, and the complete set of unknown parameters is indicated with $\boldsymbol{\Theta} = \begin{bmatrix} \boldsymbol{\theta}_1^\mathsf{T}, \boldsymbol{\theta}_2^\mathsf{T} \cdots, \boldsymbol{\theta}_{N_{\mathrm{bs}}}^\mathsf{T} \end{bmatrix}^\mathsf{T} \in \Gamma$, where $\Gamma = \mathbb{C}^{N_{\mathrm{bs}}} \times \mathbb{R}^{3N_{\mathrm{bs}}}$ is the considered parameter space.

Ignoring the terms that are not relevant for the estimation, the likelihood function of the received signal in (9) is

$$f(\tilde{\mathbf{y}}|\mathbf{\Theta}, \mathbf{x}) = \prod_{i=1}^{N_{\text{bs}}} \exp\left(-\frac{1}{\sigma_{\nu}^{2}} \|\mathbf{y}_{i} - h_{i}\mathbf{G}(f_{D,i}, \tau_{i}, \phi_{i})\mathbf{x}_{i}\|^{2}\right)$$

and the corresponding log-likelihood function is

$$l(\tilde{\mathbf{y}}|\boldsymbol{\Theta}, \mathbf{x}) = -\frac{1}{\sigma_{\nu}^2} \sum_{i=1}^{N_{\text{bs}}} \left\| \mathbf{y}_i - h_i \mathbf{G}(f_{D,i}, \tau_i, \phi_i) \mathbf{x}_i \right\|^2.$$
 (10)

From (10), an ML estimation problem can be formulated to estimate the unknown parameters in Θ :

$$\widehat{\mathbf{\Theta}}_{\mathrm{ML}} = \underset{\mathbf{\Theta} \in \Gamma}{\arg\max} \ l(\tilde{\mathbf{y}}|\mathbf{\Theta}, \mathbf{x}). \tag{11}$$

It is worth noting that the estimate of each complex channel coefficient h_i depends solely on the received signal \mathbf{y}_i at the i-th BS. Under this premise, the ML estimator of the i-th channel coefficient, \hat{h}_i , is given by (25) in the Appendix. By substituting \hat{h}_i into (10) and applying the same steps as outlined in the Appendix, (11) can be rewritten as

$$\begin{aligned} \left[\widehat{f}_{\mathrm{D},1}, \widehat{\tau}_{1}, \widehat{\phi}_{1}, \dots, \widehat{f}_{\mathrm{D},N_{\mathrm{bs}}}, \widehat{\tau}_{N_{\mathrm{bs}}}, \widehat{\phi}_{N_{\mathrm{bs}}} \right] &= \\ &= \underset{\{f_{\mathrm{D},i},\tau_{i},\phi_{i}\}}{\operatorname{arg\,max}} \sum_{i=1}^{N_{\mathrm{bs}}} \frac{|\mathbf{y}_{i}^{\mathsf{H}} \mathbf{G}(f_{\mathrm{D},i},\tau_{i},\phi_{i}) \mathbf{x}_{i}|^{2}}{\left\| \mathbf{G}(f_{\mathrm{D},i},\tau_{i},\phi_{i}) \mathbf{x}_{i} \right\|^{2}} \end{aligned}$$

where $\Omega = \mathbb{R}^{3N_{\rm bs}}$ is the search space. The ML estimation in (12) can be further simplified as derived below.

Referring to Fig. 1, the relationship between \mathbf{p}_i and \mathbf{p} is given by the following transformation

3

$$\{x_i = x_i' \cos(\vartheta_i) + y_i' \sin(\vartheta_i); y_i = -x_i' \sin(\vartheta_i) + y_i' \cos(\vartheta_i)\}$$
(13)

where $x_i' = x - x_{\rm bs}^{(i)}$ and $y_i' = y - y_{\rm bs}^{(i)}$, while ϑ_i is the counterclockwise rotation angle of the *i*-th reference system with respect to the common one. The local coordinate of the target, \mathbf{p}_i , are, in turn, related to the unknown parameters (τ_i, ϕ_i) , through

$$\left\{\phi_i = \arctan(y_i/x_i); \ \tau_i = \frac{2}{c}\sqrt{x_i^2 + y_i^2}\right\}.$$
 (14)

Therefore, the parameters $\{\tau_i, \phi_i\}_{i=1}^{N_{\rm bs}} \subset \Theta$ can be expressed as a function of the target position \mathbf{p} in the common reference system, i.e., $\{\tau_i(\mathbf{p}), \phi_i(\mathbf{p})\}_{i=1}^{N_{\rm bs}}$. The ML estimator in (12) can then be rewritten as

$$\left[\hat{f}_{\mathrm{D},1},\ldots,\hat{f}_{\mathrm{D},N_{\mathrm{bs}}},\hat{\mathbf{p}}\right] = \tag{15}$$

$$= \underset{\left[\{f_{\mathrm{D},i}\}_{i=1}^{N_{\mathrm{bs}}},\mathbf{p}\right] \in \Pi}{\operatorname{arg\,max}} \sum_{i=1}^{N_{\mathrm{bs}}} \frac{|\mathbf{y}_{i}^{\mathsf{H}}\mathbf{G}(f_{\mathrm{D},i},\tau_{i}(\mathbf{p}),\phi_{i}(\mathbf{p}))\mathbf{x}_{i}|^{2}}{\left\|\mathbf{G}(f_{\mathrm{D},i},\tau_{i}(\mathbf{p}),\phi_{i}(\mathbf{p}))\mathbf{x}_{i}\right\|^{2}}$$

with $\Pi = \mathbb{R}^{N_{\rm bs}+2}$ the new search space.

Lastly, if for a given \mathbf{p} , or (τ_i, ϕ_i) pair, the estimate of the Doppler shift, $\widehat{f}_{\mathrm{D},i}$, can be computed at each BS (e.g., through a coarse estimation procedure or by exploiting information from tracking algorithms) and then replaced in (15), the cooperative ML target position estimation for an ISAC network composed of N_{bs} BS can be computed as³

$$\widehat{\mathbf{p}} = \underset{\mathbf{p} \in \mathbb{R}^2}{\operatorname{arg \, max}} \sum_{i=1}^{N_{\text{bs}}} \frac{|\mathbf{y}_i^{\mathsf{H}} \mathbf{G}(\widehat{f}_{\mathrm{D},i}, \tau_i(\mathbf{p}), \phi_i(\mathbf{p})) \mathbf{x}_i|^2}{\|\mathbf{G}(\widehat{f}_{\mathrm{D},i}, \tau_i(\mathbf{p}), \phi_i(\mathbf{p})) \mathbf{x}_i\|^2}.$$
 (16)

B. Numerical Evaluation of Cooperative Maximum Likelihood

As mentioned, solving (16) requires an initial estimation of the Doppler shifts $\{f_{\mathrm{D},i}\}_{i=1}^{N_{\mathrm{bs}}}$, achieved by evaluating (12) within the defined search space Ω . For a cooperative ISAC system with $N_{\mathrm{bs}} \geq 2$ BSs, this ML estimation operates in a continuous search space of dimension ≥ 6 , leading to considerable complexity. To simplify computation, we employ an approximate method: breaking down the estimation into N_{bs} independent problems, each in a 3D search space $\tilde{\Omega} \subset \Omega$.

Assuming a prior target detection phase has identified a RoI as in [12], the search space for $\{\tau_i,\phi_i\}_{i=1}^{N_{\rm bs}}$ in (12) is limited to range of values within the RoI (see Fig. 1). Doppler shifts $\{f_{{\rm D},i}\}_{i=1}^{N_{\rm bs}}$ are similarly restricted, based on the scenario. Hence, we define a discrete set of tuples $(f_{{\rm D},i},\tau_i,\phi_i)\in\tilde{\Omega}$ as

$$\tilde{\Omega} = \{f_{\mathrm{D},i}^{\mathrm{min}},...,f_{\mathrm{D},i}^{\mathrm{max}}\} \times \{\tau_{i}^{\mathrm{min}},...,\tau_{i}^{\mathrm{max}}\} \times \{\phi_{i}^{\mathrm{min}},...,\phi_{i}^{\mathrm{max}}\}$$

with steps $\delta f_{\rm D}=c_{f_{\rm D}}\Delta f_{\rm D},\ \delta \tau=c_{\tau}\Delta \tau,\ {\rm and}\ \delta \phi=c_{\phi}\Delta \Phi,$ being $\Delta f_{\rm D}=1/(NT)$ and $\Delta \tau=1/(M\Delta f)$ the system resolution in Doppler and delay, respectively, and $\Delta \Phi$ the beamwidth at 0 degrees, while $c_{f_{\rm D}},c_{\tau},c_{\phi}\in(0,1]$ are factors used to control the desired accuracy of parameter estimation.

³Interestingly, (16) also applies to OFDM, where the effective channel matrix G can be represented as in [12, Equation (23)].

Once Doppler shifts $\{\widehat{f}_{\mathrm{D},i}\}_{i=1}^{N_{\mathrm{bs}}}$ are estimated, (16) can then be used to compute $\widehat{\mathbf{p}}$. As before, the search is discretized within the RoI by defining a discrete set of common coordinates as $\{x_{\min},...,x_{\max}\} \times \{y_{\min},...,y_{\max}\}$, with steps Δx and Δy , respectively, chosen to achieve the desired accuracy.

Notably, (16) can be interpreted as a summation of $N_{\rm bs}$ radar maps in the x-y plane, computed within the RoI, as shown in Fig. 1.

C. Cramér-Rao Lower Bound Derivation

Let us define $\mu_i = h_i \mathbf{G}(f_{\mathrm{D},i}, \tau_i, \phi_i) \mathbf{x}_i \in \mathbb{C}^{MNN_{\mathrm{R}} \times 1}$ as the vector of mean values of the received signal \mathbf{y}_i at the *i*-th BS. The CRLB on the estimation of the unknown parameters $\boldsymbol{\theta}_i$, is given by

$$\mathbb{V}\{\hat{\theta}_{i,q}\} \ge \mathrm{CRB}(\theta_{i,q}) = \left[\mathcal{I}^{-1}(\boldsymbol{\theta}_i)\right]_{q,q} \quad q = 1, \dots, \mathrm{card}(\boldsymbol{\theta}_i)$$

where $\hat{\theta}_{i,q}$ is the estimate of the q-th parameter contained in θ_i , and $[\mathcal{I}^{-1}(\theta_i)]_{q,q}$ represents the q-th element on the main diagonal of the inverse of the Fisher information matrix (FIM) $\mathcal{I}(\theta_i)$. The vector $\boldsymbol{\mu}_i$ can be reshaped into a 3D array with elements $\mu_i[k,l,j]$, indexed by (k,l,j), corresponding to dimensions $(M\times N\times N_{\mathrm{R}})$, respectively. The generic qp-th element of $\mathcal{I}(\theta_i)$ can then be computed as [10], [13]

$$\left[\mathcal{I}(\boldsymbol{\theta}_{i})\right]_{q,p} = \frac{2}{\sigma_{\nu}^{2}} \mathfrak{Re} \left\{ \sum_{k,l,j} \left(\frac{\partial \mu_{i}[k,l,j]}{\partial \theta_{i,q}} \right)^{*} \left(\frac{\partial \mu_{i}[k,l,j]}{\partial \theta_{i,p}} \right) \right\}$$
(17)

where

$$\mu_i[k,l,j] = \beta_i e^{j\varphi_i} b_j(\phi_i) \sum_{k'=0}^{M-1} \sum_{l'=0}^{N-1} \mathbf{\Psi}_{l,l'}[k,k'] x_i[k',l'] \quad (18)$$

with $b_j(\phi)$ the j-th element of the array response vector $\mathbf{b}(\phi)$.⁴ The vector $\boldsymbol{\theta}_i$ can be partitioned as $\boldsymbol{\theta}_i = [\boldsymbol{\theta}_{i,1}^\mathsf{T}, \boldsymbol{\theta}_{i,2}^\mathsf{T}]^\mathsf{T}$, with $\boldsymbol{\theta}_{i,1} = [\beta_i, \varphi_i, f_{\mathrm{D},i}]^\mathsf{T}$, $\boldsymbol{\theta}_{i,2} = [\tau_i, \phi_i]^\mathsf{T}$, which induces the partition of the FIM into the matrices $\mathbf{A} \in \mathbb{R}^{3\times3}$, $\mathbf{B} \in \mathbb{R}^{3\times2}$, and $\mathbf{C} \in \mathbb{R}^{2\times2}$, as $\boldsymbol{\mathcal{I}}(\boldsymbol{\theta}_i) = \begin{bmatrix} \mathbf{A} & \mathbf{B} \\ \mathbf{B}^\mathsf{T} & \mathbf{C} \end{bmatrix}$. Then, the equivalent Fisher information (EFIM) is [14], [15]: $\boldsymbol{\mathcal{I}}(\boldsymbol{\theta}_{i,2}) = \mathbf{C} - \mathbf{B}^\mathsf{T} \mathbf{A}^{-1} \mathbf{B}$.

Considering that each BS independently observes the target parameters, the FIM for cooperative position estimation is given by [14], [15]

$$\mathcal{I}_{e}(\mathbf{p}) = \sum_{i=1}^{N_{BS}} \mathbf{J}_{n}^{\mathsf{T}} \Big(\mathbf{J}_{m}^{\mathsf{T}} \mathcal{I}_{e}(\boldsymbol{\theta}_{i,2}) \mathbf{J}_{m} \Big) \mathbf{J}_{n}$$
 (19)

where \mathbf{J}_{m} and \mathbf{J}_{n} represent the Jacobian of the transformations $(r_i, \phi_i) \rightarrow \mathbf{p}_i$, and $\mathbf{p} \rightarrow \mathbf{p}_i$, respectively, whose definition, considering (14) and (13), are as follows

$$\mathbf{J}_{\mathrm{m}} \triangleq \begin{bmatrix} \frac{\partial \tau_{i}}{\partial x_{i}} & \frac{\partial \tau_{i}}{\partial y_{i}} \\ \frac{\partial \phi_{i}}{\partial x_{i}} & \frac{\partial \phi_{i}}{\partial y_{i}} \end{bmatrix}, \qquad \mathbf{J}_{\mathrm{n}} \triangleq \begin{bmatrix} \frac{\partial x_{i}}{\partial x} & \frac{\partial x_{i}}{\partial y} \\ \frac{\partial y_{i}}{\partial x} & \frac{\partial y_{i}}{\partial y} \end{bmatrix}. \tag{20}$$

After computing (20), the CRLB of position estimate is determined as $\mathbb{V}\{e_{\mathrm{p}}\} \geq \mathrm{CRB}(\mathbf{p}) = \mathrm{Tr}(\mathcal{I}_{\mathrm{e}}^{-1}(\mathbf{p}))$. The PEB is then defined as

$$PEB \triangleq \sqrt{CRB(\mathbf{p})}.$$
 (21)

TABLE I JSC NETWORK PARAMETERS

Parameters	Symbols	Values
Number of Tx and Rx antennas	$N_{\rm T}$, $N_{\rm R}$	16
Antenna element gain	G	1
Tx beamwidth / Beamforming gain	- / G _b	40° / ∼ 4.1 dB
Total transmit power	P_{T}	30 dBm
Carrier frequency	$f_{\rm c}$	60 GHz
Time slots / Active subcarriers	N / M	50 / 96
Subcarrier spacing / Time slot duration	$\Delta f / T$	1 MHz / 1 μs
Noise power spectral density	N_0	4 · 10 ⁻²⁰ W/Hz
Target radar cross-section	σ	1 m ²
Region-of-interest / pixel size	RoI / $(\Delta x \times \Delta y)$	$16 \text{ m}^2 / (0.02 \times 0.02) \text{ m}^2$

IV. NUMERICAL RESULTS

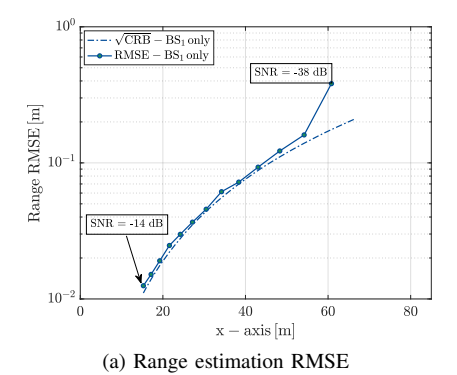
The proposed cooperative ML estimation framework is validated through numerical simulation, varying the number of BSs, $N_{\rm bs}$, up to 3, in the scenario shown in Fig. 1 with system parameters listed in Table I. The three BSs are placed at the corners of an 85 m square area, numbered as in Fig. 1, with the origin of the common reference system in \mathcal{O}_1 . The following rotation angles, $[\vartheta_1, \vartheta_2, \vartheta_3] = [\pi/4, 5\pi/4, 3\pi/4]$, are considered. The point-like target moves along the diagonal connecting BS_1 and BS_2 . As outlined in Section III-B, a two-stage estimation, consisting of a coarse and a refined estimation within a defined RoI, is performed. For the coarse estimation, the search steps $\delta f_{\rm D}$, $\delta \tau$, $\delta \phi$ are computed with $c_{\tau}=1,\,c_{f\mathrm{D}}'=c_{\phi}'=0.25,\,\mathrm{with}\,\,\Delta\Phi\simeq0.1108\,\mathrm{rad}.$ The matrix Ψ used to compute G in (12) and (16) is calculated based on the approximation method illustrated in [10], specifically using $N_{\text{lobe}} = 5$ with reference to [10, Equation (45)].

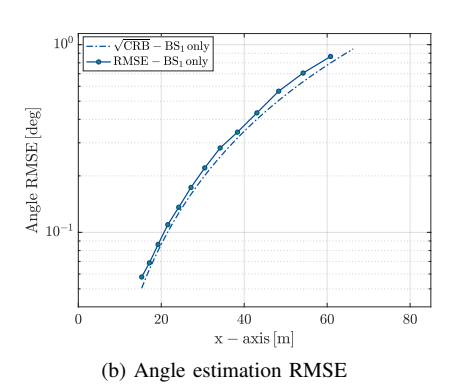
Sensing performance is evaluated in terms of RMSE of range, angle, and position estimates. For a given vector of parameters \mathbf{q} this is computed as RMSE = $\sqrt{\frac{1}{N_{\mathrm{MC}}}\sum_{m=1}^{N_{\mathrm{MC}}}\|\hat{\mathbf{q}}_m - \mathbf{q}\|^2}$, being $N_{\mathrm{MC}} = 500$ the number of Monte Carlo iterations. The results are shown in Fig. 2, where RMSEs alongside the corresponding CRLBs are plotted against varying target's position. Since the target moves along the square's diagonal y = x, its position in the common reference system is represented here by its x coordinate only.

Fig. 2a, Fig. 2b, and blue curve in Fig. 2c show the range, angle, and position estimates RMSE, respectively, when BS₁ alone performs sensing. As expected, the RMSEs linearly increase as the targets moves away from BS₁, reaching a maximum of 1.34 m in position error, for the considered set of target coordinates. In contrast, examining all curves in Fig. 2c highlights the benefits of cooperative ML target position estimation: for $N_{\rm bs} \geq 2$ the position estimation error is reduced to a maximum of 0.3 m and 0.1 m with 2 and 3 BSs respectively. As a further example, when x=48.3 m the RMSE is equal to 0.69 m, 0.27 m, and 0.1 m when considering 1, 2 and 3 BSs, respectively.

Notably, for the considered single-target scenario, the proposed cooperative ML framework achieves performance that closely matches the corresponding PEB, underscoring the effectiveness of cooperative ML estimation.

⁴By substituting (18) into (17), the necessary partial derivatives of Ψ can be found in closed form in [10].





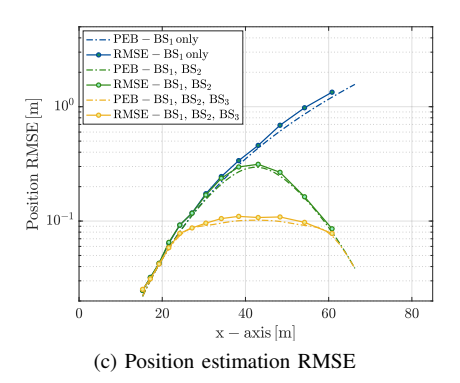


Fig. 2. RMSE and $\sqrt{\text{CRB}}$ for estimates of range \hat{r} (a), angle $\hat{\phi}$ (b), and position (c) as the target moves along the diagonal line between BS₁ and BS₂ within the square area shown in Fig. 1. The x-axis represents the target's position – in the common reference system – along the diagonal, where y=x. Results in (a) and (b) are related to BS₁ only, while (c) shows outcomes as N_{bs} varies up to 3.

V. CONCLUSION

This letter proposed a cooperative ML framework for target position estimation in MIMO OTFS-based ISAC networks with multiple cooperating monostatic BSs. Results demonstrated the significant advantages of inter-BS cooperation: specifically, the cooperative approach achieved a position estimation error below 10 cm with three BSs, a sevenfold improvement over single BS configurations. Furthermore, the proposed framework closely approached the theoretical PEB, underscoring its efficiency. These findings highlight the potential of cooperative ISAC for significantly enhancing localization accuracy over single BS setups.

APPENDIX

A. Maximum Likelihood Estimation

Considering a given BS and omitting its index i, after a few manipulations, (10) takes on the form

$$l(\mathbf{y}|\boldsymbol{\theta}, \mathbf{x}) = -\frac{1}{\sigma_{\nu}^2} \left(\beta^2 \big\| \mathbf{G} \mathbf{x} \big\|^2 + \big\| \mathbf{y} \big\|^2 - 2\beta \mathfrak{Re}\{e^{j\varphi} \mathbf{y}^{\mathsf{H}} \mathbf{G} \mathbf{x}\}\right).$$

Now, ignoring those constant positive terms that do not contribute to the estimation, the log-likelihood reduces to

$$\tilde{l}(\mathbf{y}|\boldsymbol{\theta}, \mathbf{x}) = 2\beta \mathfrak{Re}\{e^{j\varphi}\mathbf{y}^{\mathsf{H}}\mathbf{G}\mathbf{x}\} - \beta^{2} \|\mathbf{G}\mathbf{x}\|^{2}.$$
 (22)

From (22) the vector of unknown parameters θ can be estimated by maximizing the log-likelihood as

$$\widehat{\boldsymbol{\theta}}_{\mathrm{ML}} = \underset{[\beta, \varphi, f_{\mathrm{D}}, \tau, \phi]}{\arg \max} \, \widetilde{l}(\mathbf{y} | \boldsymbol{\theta}, \mathbf{x}). \tag{23}$$

Since $\beta > 0$, the phase φ of the complex channel coefficient h that maximizes $\tilde{l}(\mathbf{y}|\boldsymbol{\theta},\mathbf{x})$ is $\hat{\varphi} = -\angle \mathbf{y}^{\mathsf{H}}\mathbf{G}\mathbf{x}$ and by replacing it in (22), this can be rewritten as

$$\tilde{l}(\mathbf{y}|\boldsymbol{\theta}, \mathbf{x}) = 2\beta |\mathbf{y}^{\mathsf{H}} \mathbf{G} \mathbf{x}| - \beta^2 ||\mathbf{G} \mathbf{x}||^2.$$
 (24)

The value of β which maximizes the likelihood function can be easily obtained and used for $\hat{h}=\hat{\beta}e^{j\hat{\phi}}$, as follows

$$\widehat{\beta} = \frac{|\mathbf{y}^{\mathsf{H}}\mathbf{G}\mathbf{x}|}{\|\mathbf{G}\mathbf{x}\|^{2}}, \qquad \widehat{h} = \frac{\mathbf{x}^{\mathsf{H}}\mathbf{G}^{\mathsf{H}}\mathbf{y}}{\|\mathbf{G}\mathbf{x}\|^{2}}.$$
 (25)

Lastly, by plugging $\widehat{\beta}$ into (24), solving (23) reduces to

$$\left[\widehat{f}_{\mathrm{D}}, \widehat{\tau}, \widehat{\phi}\right] = \underset{\left[f_{\mathrm{D}}, \tau, \phi\right] \in \mathbb{R}^{3}}{\arg \max} \frac{|\mathbf{y}^{\mathsf{H}} \mathbf{G} \mathbf{x}|^{2}}{\|\mathbf{G} \mathbf{x}\|^{2}}.$$
 (26)

REFERENCES

- Z. Wei et al., "Integrated sensing and communication enabled multiple base stations cooperative sensing towards 6g," *IEEE Network*, vol. 38, no. 4, pp. 207–215, July 2024.
- [2] Y. Xu, L. Xie, D. Xu, and S. Song, "Fundamental limits and base station selection for collaborative sensing in perceptive mobile networks," in *Proc. IEEE Int. Mediterranean Conf. on Commun. and Netw. (Medit-Com)*, Dubrovnik, Croatia, Sep. 2023, pp. 97–102.
- [3] Z. Wei et al., "Symbol-level integrated sensing and communication enabled multiple base stations cooperative sensing," *IEEE Trans. Veh. Technol.*, vol. 73, no. 1, pp. 724–738, Jan. 2024.
- [4] P. Gao, L. Lian, and J. Yu, "Cooperative ISAC with direct localization and rate-splitting multiple access communication: A pareto optimization framework," *IEEE J. Sel. Areas Commun.*, vol. 41, no. 5, pp. 1496–1515, May 2023.
- [5] M. Chen, M.-M. Zhao, A. Liu, M. Li, and Q. Shi, "Joint node selection and resource allocation optimization for cooperative sensing with a shared wireless backhaul," 2024. [Online]. Available: https://arxiv.org/abs/2405.16791
- [6] K. Meng and C. Masouros, "Cooperative sensing and communication for isac networks: Performance analysis and optimization," in *Proc. IEEE Workshop Signal Process. Adv. Wirel. Commun. (SPAWC)*, Lucca, Italy, Sep. 2024, pp. 446–450.
- [7] B. Friedlander, "On transmit beamforming for mimo radar," *IEEE Trans. Aerosp. Electron. Syst.*, vol. 48, no. 4, pp. 3376–3388, Oct. 2012.
- [8] R. Hadani et al., "Orthogonal time frequency space modulation," CoRR, vol. abs/1808.00519, 2018. [Online]. Available: http://arxiv.org/abs/1808.00519
- [9] L. Gaudio, M. Kobayashi, G. Caire, and G. Colavolpe, "On the effectiveness of OTFS for joint radar parameter estimation and communication," *IEEE Trans. Commun.*, vol. 19, no. 9, pp. 5951–5965, Sep. 2020.
- [10] T. Bacchielli, L. Pucci, E. Paolini, and A. Giorgetti, "A low-complexity detector for OTFS-based sensing," Jan. 2024. [Online]. Available: http://dx.doi.org/10.36227/techrxiv.170630403.34764069/v1
- [11] S. K. Dehkordi, L. Gaudio, M. Kobayashi, G. Caire, and G. Colavolpe, "Beam-space mimo radar for joint communication and sensing with OTFS modulation," *IEEE Trans. Wireless Commun.*, vol. 22, no. 10, pp. 6737–6749, Oct. 2023.
- [12] S. K. Dehkordi, L. Pucci, P. Jung, A. Giorgetti, E. Paolini, and G. Caire, "Multistatic parameter estimation in the near/far field for integrated sensing and communication," *IEEE Trans. Wireless Commun.*, 2024.
- [13] D. Rife and R. Boorstyn, "Single tone parameter estimation from discrete-time observations," *IEEE Trans. Inf. Theory*, vol. 20, no. 5, pp. 591–598, Sept. 1974.
- [14] Y. Shen and M. Z. Win, "Fundamental limits of wideband localization—part I: A general framework," *IEEE Trans. Inf. Theory*, vol. 56, no. 10, pp. 4956–4980, Sep. 2010.
- [15] L. Pucci and A. Giorgetti, "Position error bound for cooperative sensing in MIMO-OFDM networks," in *Proc. IEEE Workshop Signal Process.* Adv. Wirel. Commun. (SPAWC), Lucca, Italy, Sep. 2024, pp. 296–300.